LAWRENCE
LIVERMORE
NATIONAL
LABORATORY

LLNL-TR-679717

Fabrication of Gamma Detectors Based on Magnetic Ag:Er Microcalorimeters[2]

S. Friedrich

November 25, 2015

Disclaimer

This work performed under the auspices of the U.S. Department of Energy by Lawrence Livermore National Laboratory under Contract DE-AC52-07NA27344.

Fabrication of Gamma Detectors Based on Magnetic Ag:Er Microcalorimeters

PI: Stephan Friedrich, Lawrence Livermore (LLNL)

Co-I: Stephen Boyd, University of New Mexico (UNM)

Robin Cantor, Star Cryoelectronics LLC (STAR Cryo)

Abstract

This report discusses the photolithographic fabrication of ultra-high resolution gamma-ray detectors based on magnetic microcalorimeters (MMCs). The MMC uses a novel Er-doped silver sensor (Ag:Er) that is expected to have higher sensitivity than the Er-doped gold (Au:Er) sensors currently in use. The MMC also integrates the first-stage SQUID preamplifier on the same chip as the MMC gamma detector to increase its signal-to-noise ratio. In addition, the MMC uses a passive Ta-Nb heat switch to replace one of the common long-term failure points in earlier detectors. This report discusses the fabrication process we have developed to implement the proposed improvements.

Project Goals

Magnetic microcalorimeters (MMCs) consist of a spin-1/2 sensor in a small magnetic field at ultra-low temperatures so that the two Zeeman levels have different energies and are unevenly occupied. Photon absorption excites electrons into the energy upper level in proportion to the photon energy, and the resulting change in magnetization is read out with a superconducting quantum interference device (SQUID) (Figure 1). Typically, one SQUID reads out two MMC pixels in a gradiometric configuration to reduce the influence of electromagnetic interference.

The goal of this project is to build an MMC gamma-ray detector array with ultra-high energy resolution<50 eV FWHM at an operating temperature of ~15 mK, and a dynamic range of ≥100 keV for nuclear safeguards [Bates 2014]. For improved sensitivity, we are developing erbium-doped silver (Ag:Er) as the preferred magnetic sensor material, although well-established erbium-doped gold (Au:Er) will be kept as a back-up option. In addition, it is desirable to increase the detector speed from currently a few counts/s per pixel to several tens of counts/s. For increased sensitivity, the MMCs will be fabricated as a 32-pixel array. The detector design must therefore be scalable, and the photolithographic fabrication must be reliable with high yield.

Design Innovations

We have incorporated several new design features into our MMC that increase device sensitivity, signal-to-noise ratio and reliability. The improvements in signal-to-noise ratio can, alternatively, be traded off for increased detector speed or increased efficiency if that is desirable for a particular application.

1) The most important innovation over competing MMC designs is to place **MMC detector and first-stage SQUID preamplifier on the same chip**. This allows us to eliminate the flux transformer and to use the Nb pick-up coil of the magnetic sensor to directly couple the MMC

signal into the SQUID preamplifier (Figure 1b). Since flux transformers can be at best 50% efficient, the integrated design boosts the signal and reduces the influence of the SQUID noise, which currently contributes ~40% to the energy resolution, by at least a factor of 2.

2) Secondly, we are fabricating **MMCs based on Ag:Er sensors**, in addition to the traditional Au:Er sensors (Figure 1b). In the 1990s, Au:Er was chosen as a sensor material because its magnetic properties were well understood and known to be acceptable, although it was known even then that gold is not ideal because of its large nuclear quadrupole moment and thus increased heat capacity. Silver, on the other hand, consists of the two spin ½ isotopes ^{107}Ag and ^{109}Ag without a nuclear quadrupole moment, and Ag:Er MMCs will therefore have a higher energy resolution because no energy is lost into the nuclear spin system.

3) In addition, we have integrated metallic AuPd pads into our SQUID preamplifiers to prevent the energy dissipation in the shunt resistors from heating the electrons above the cryostat temperature. These "**cooling fins**" keep the electrons in the SQUID shunts at the temperature of the cryostat and thus reduce the SQUID noise to its lowest value.

4) Also, a **superconducting capping layer** has been added above the Ag:Er sensor to confine the magnetic field to the sensor region and thus to increase the field at the location of the Er dopants. This improves the coupling between magnetic sensor and preamplifier, increases the γ-induced signal per magnetization change of the paramagnet and thus again improves the energy resolution of the detectors [Boyd 2009].

5) Finally, for increased reliability we have replaced the AuPd heater of our persistent current switch with a **passive heat switch** based on Ta/Nb with a critical temperature T_C = 5.5K (Figure 2). Our field-generating loop will now automatically switch to zero resistance once the heat switch cools below T_C, rather than requiring activation with a current pulse through a resistive AuPd heater, which was prone to failure after months of operation (Figure 3).

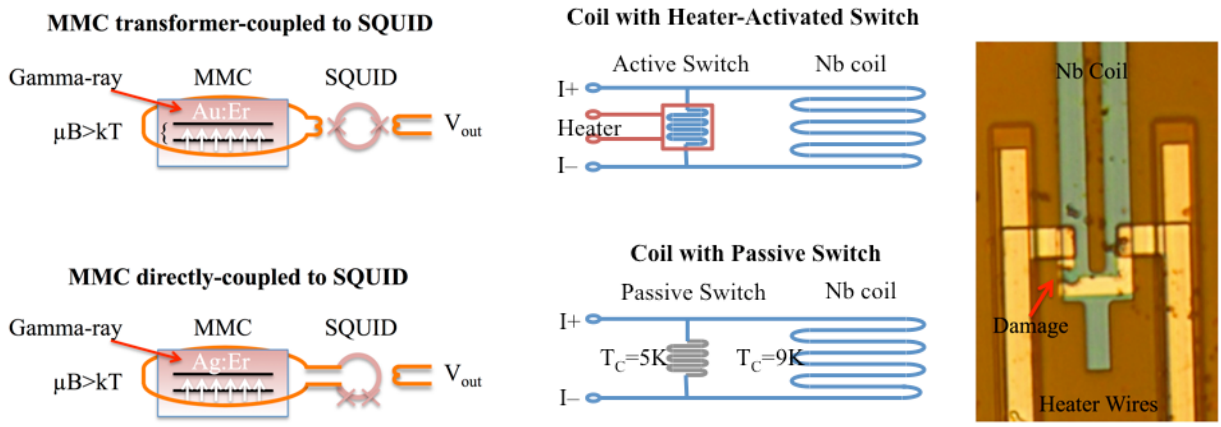

Figure 1 (left): Traditional MMC readout with transformer-coupling to the SQUID preamplifier (top) The ability to fabricate MMC and SQUID on the same chip at STAR Cryo allows us to directly couple the MMC signal into the SQUID loop (bottom). Figure 2 (center): Traditional magnetizing coil with active heat switch (top), compared to the UNM design with a passive heat switch (bottom). Figure 3 (right): Damaged heat switch due to repeated current pulses in an earlier LLNL device after 3 months of operation.

Detector Simulations

We have performed extensive numerical simulations of the MMC performance for different device geometries. Specifically, we have calculated the magnetic field distribution inside the Ag:Er sensor and the achievable signal for different magnetizing coil geometries (meander vs. spiral), coil thickness and line spacing, sensor thickness and erbium concentration, with and without a superconducting cap. The simulations were written in Comsol and Matlab, and were performed at the University of New Mexico Center for Supercomputing.

As an example, Figure 4 shows the calculated magnetic field distribution in a Ag:Er sensor with a Nb cap and a magnetizing coil with spiral geometry. This is a simulation for a two-coil geometry, with a lower coil with 9 µm leads that carries a high current to magnetize the Er dopants, and an upper coil with 5 µm leads that forms part of the SQUID loop to read out the gamma-ray signal. This novel two-coil design electrically isolates the SQUID preamplifier from the magnetizing circuit to reduce pick-up from crosstalk. Importantly, and somewhat surprisingly, the simulations show that the performance penalty for the two-coil design is only a few percent, because most of the magnetic field lines surround both coils. They also show how well the Nb cap confines the magnetic field to the Ag:Er sensor region to maximize the signal.

These simulations allow quantifying the improvements that the MMC designs with Nb caps and direct coupling to the SQUID offer over the traditional MMC designs without Nb cap and transformer coupling. The new design increases the signal-to-noise ratio by a factor of ~4, and this improvement can be achieved at lower applied field strength (Figure 5). This reduces the need for high magnetizing currents and provides a safety margin against flux trapping in the Nb layers. In addition, further benefits can probably be obtained with a thicker paramagnetic sensor, subject to the constraints of photolithographic fabrication.

So far, the material parameters of the simulations are only based on literature values. We have therefore included several test structures on the photomasks to measure important material and device parameters such as film purity, critical currents and thermal conductances. The measured quantities will be fed back into future simulations for design optimization.

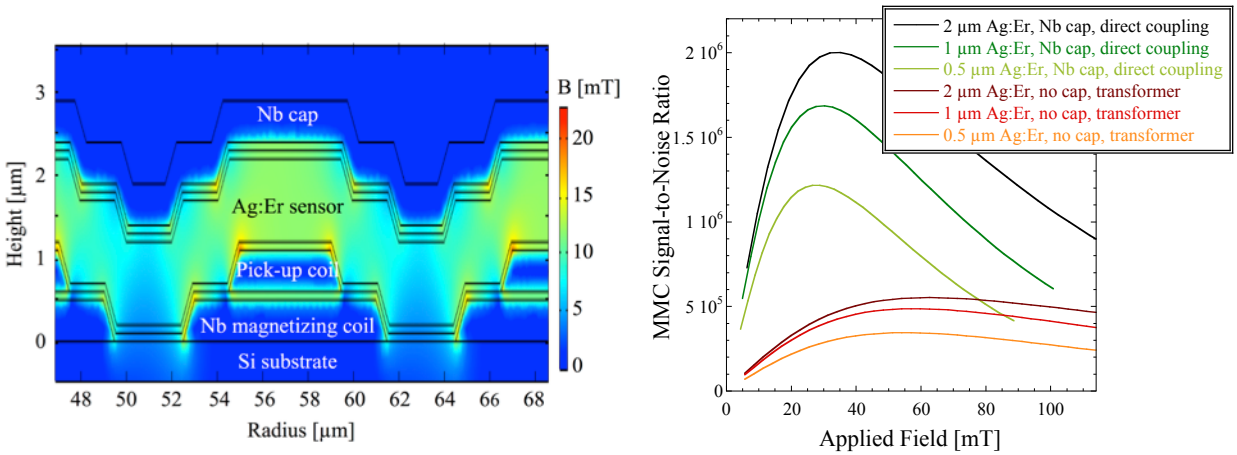

Figure 4 (left): Simulation of the magnetic field due to current in the Nb magnetizing coil in the Ag:Er sensor. The insulating SiO_2 layers between the different components are not labeled, but included in the simulations. The Nb cap on top of the Ag:Er confines the B-field to the sensor region. Figure 5 (right): Simulated signal-to-(SQUID) noise ratio at 60 keV for Ag:Er MMCs with different sensor thicknesses and different coupling geometry (traditional meander geometry with transformer-coupling vs. spiral geometry with novel direct coupling).

SQUID Preamplifier Fabrication

The readout SQUID amplifier is fabricated first, because its tunnel junctions are the most sensitive part of the device, and it is standard practice for best performance to deposit and pattern the junction layers first. The SQUID fabrication is based on STAR Cryo's proprietary Delta 1000 process, but has been adapted to provide the circuitry to generate a magnetic field for the MMC and to pick-up gamma-ray signals. For example, the Nb film that forms the base layer of the tunnel junctions in the SQUID has been made very thick so that it can carry high currents and also be used for the magnetizing coil (Figure 6).

The SQUIDs are fabricated on standard 4" Si wafers with 400 nm thermal oxide (the orientation, doping, and resistivity of the starting wafers are not critical for this application). The Nb / Al-AlOx/ Nb trilayer is sputter-deposited in a single vacuum cycle with careful monitoring of the vacuum conditions and deposition parameters for maximum reproducibility of the junction characteristics. The 600 nm Nb base layer is uncommonly thick, because it also forms the magnetizing coil for the MMC and must therefore be able to carry currents >100 mA. The 9 nm aluminum film is oxidized in a load lock using pure oxygen to form the tunnel barrier, and the oxygen exposure is adjusted to achieve a critical current density of ~50 A/cm^2. The top Nb electrode is 60 nm thick. The first etch of the trilayer is timed to go through the top Nb electrode and the tunnel barrier to define the junction area. A second etch defines the Nb base electrode and the geometry of the magnetizing coil for the MMC detector (Figure 6).

One problem that we (and other groups) have experienced in the past is the reliability of the heat switch that is needed to freeze a permanent current in the superconducting Nb coil below the MMC and magnetize the Er dopants. Traditionally, this heat switch consists of a short section of resistive material on top of the Nb coil, and is activated by applying a short ~100 mA current pulse to heat a section of the Nb above its critical temperature T_C. Once the Nb cools again below T_C, any current in the circuit is trapped in the coil, and the external power supply can be turned off. While this design works, repeated current pulsing can damage the heat switch until it eventually delaminates from the Nb loop and breaks (Figure 3). We have therefore replaced the resistive heat switch with a passive heat switch that consists of a 10 nm Nb / 167 nm Ta bilayer, with the thicknesses chosen for a critical temperature $T_C \approx 5.5$ K. A current is applied to the Nb coil, and as the detector cools below $T_C \approx 5.5$ K, the heat switch loses its resistance so that the current is trapped in the Nb loop and the external power supply can be turned off. This passive Ta-Nb heat switch is deposited immediately after the SQUID junctions and defined by lift-off.

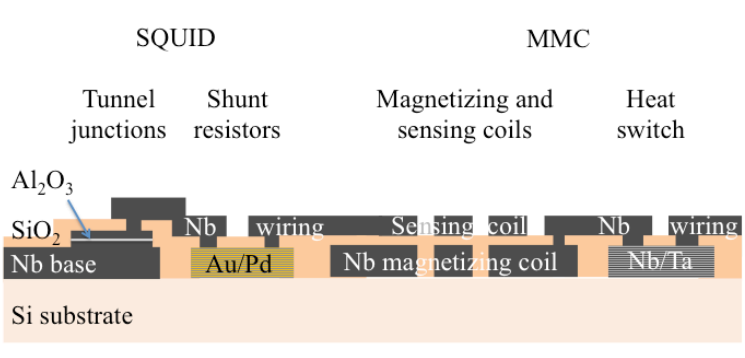

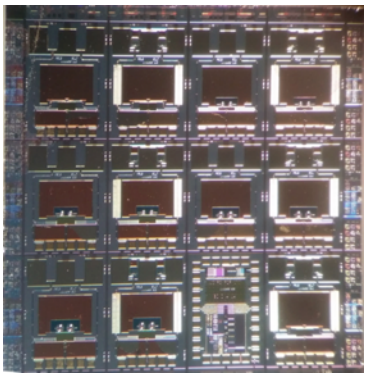

Figure 6 (right): Schematic cross section of the SQUID wafer during fabrication. Figure 7 (Left): After SQUID fabrication, the 4" wafer is diced into 1 cm^2 chips for integration of the MMC detector.

Next, a 200 nm thick blanket layer of high-quality SiO_2 is deposited by plasma-enhanced chemical vapor deposition (PECVD) to isolate the junction edges and to cover the base wiring and persistence switch. Vias through the oxide are opened to be able to make electrical contacts to the junction electrodes and the persistence switch. The vias are patterned using a reactive ion etch (RIE) process to achieve sloped edge profiles in the oxide, which we have found to be essential to achieve high critical current densities around the via edges. The subsequent Nb wiring layer also needs to carry the high magnetizing current (a gradiometric MMC requires a ”figure-8” superconducting loop for magnetization), and this in turn requires a high interface quality between the different Nb films. Before depositing the first Nb wiring layer, we therefore plasma clean the exposed Nb or Ta-Nb film surface to eliminate any contact resistance. The Nb wiring layer is then sputter-deposited to a thickness of ~300 nm and patterned using lift-off. It also forms the sensing coil that is used to pick up the magnetic signal of the MMC detector (Figure 6). This selective niobium etch process (SNEP) has proven to be very robust and very reliable, with yields at final test of well over 90%.

A 2 nm Ti adhesion layer and resistive AuPd film ~210 nm thick are deposited next and patterned by lift-off. The patterned AuPd film forms the resistive shunts of the SQUID and the attached cooling fins to keep the shunts at the cryostat base temperature. We then deposit an additional SiO_2 insulator by PECVD and a second Nb wiring layer. Finally, a 300 nm Au pad metallization layer is deposited and patterned by lift-off to form the thermal path and the bonding pads for gold ribbon wire bonds to make thermal connections to the detector. It contains a thin section to provide a thermal bottleneck so that we can adjust the signal decay time (Figure 9).

The finished 4” wafer with the SQUID preamplifier is then cut into ~1 cm^2 dies that are processed individually to integrate the MMC detector (Figure 7). Since the Nb sensing coil forms part of the SQUID loop, it is already fabricated as part of the SQUID design.

MMC Gamma Detector Fabrication

We initially deposit a SiO_2 insulator on top of the sensing coil by plasma-enhanced physical vapor deposition (PECVD) to electrically isolate the MMC sensor from the underlying Nb coils. STAR Cryo’s PECVD process is of very high quality and allows us to limit the thickness of the SiO_2 insulator to 100 nm without creating pinholes. For comparison, other groups require a 200 nm thick SiO_2 insulator that reduces the coupling between the Ag:Er sensor and the Nb sensing coil and thus the signal size.

The magnetic Er-doped silver (Ag:Er) sensor is subsequently deposited in a dedicated sputter chamber to avoid contaminating other processes with magnetic erbium ions. Ag:Er is an unusual sensor material for which sputter targets are not commercially available. As part of the predecessor proposal, UNM has therefore fabricated several 1” diameter Ag:Er targets with different Er concentrations and measured their magnetic properties. For this project, we are using a Ag:Er target with an Er concentration of 1000 ppm. We can adjust the Er concentration in the Ag:Er sensor by co-sputtering with a pure silver target [Jaeckel 2012]. This reduction suppresses the 1/f noise due to magnetic interactions between the Er dopants, and prevents the formation of magnetic domains that no longer change their spin in response to gamma rays. The 1” diameter of the targets and the substrate rotation during deposition ensure that the Ag:Er sensor is deposited uniformly over the 1 cm^2 area of the 12 chips on the die that we process per batch. The sensor is patterned by lift-off.

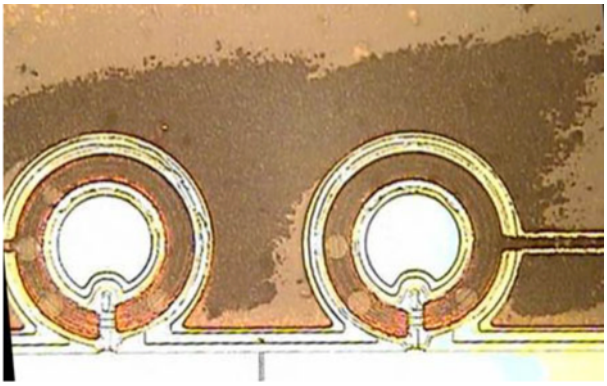

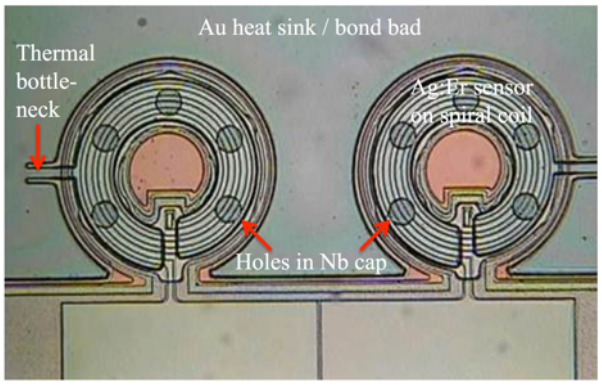

Figure 8 (left): Poor photolithographic definition of the structures on top of the Ag:Er sensor caused by roughness and UV reflectivity of the Ag surface. Figure 9 (right): Well-defined structures after deposition of 60 nm of Au onto the Ag:Er sensor. The small Au path between the Ag:Er sensor and the Au heat sink forms a bottleneck in the cool-down of the sensor and can be adjusted photolithographically to set the MMC signal decay time.

We were initially surprised to discover that photolithographic patterning of structures on top of the Ag:Er sensor was of very poor quality. We eventually traced the problem to the fact that Ag has a certain surface roughness *and* that it reflects the UV light used to pattern the photoresist on top of it. The diffusive reflection exposes the photoresist to UV light in regions to the side of the photomask and therefore washes out the structures used to pattern subsequent features (Figure 8). Gold, on the other hand, does not reflect UV light – its golden color, after all, is due to reflection of red, orange and yellow wavelengths and the absorption of green, blue and violet. We are therefore now depositing a 60 nm Au layer on top of the Ag:Er absorber to absorb UV light that passes through the photoresist layer on top of it. This Au layer has the additional advantage that we no longer need to ion mill the Ag:Er to remove its surface oxide and ensure good thermal contact with the Au absorber.

(Since the gold layer must be deposited in the same vacuum cycle immediately after the Ag:Er absorber, the gold target is currently replacing the Ag target that we use for co-sputtering. Our current Ag:Er MMCs therefore have a comparably high Er concentration of 1000 ppm. To retain the ability for co-sputtering to reduce the Er concentration, we are investigating options to add at least one more sputter gun to our deposition chamber in FY17.)

We then have the option to deposit an SiO_2 insulator on top of the Ag:Er to separate it electrically from the subsequent Nb cap. This superconducting cap helps to confine the magnetic field to the region of the Ag:Er sensor (thereby increasing the signal) and to reduce the parasitic inductance (thereby decreasing the noise of the MMC) (Figures 4, 5). There is some discussion in the field whether an insulator between the sensor and the Nb cap is advantageous, and our ability to fabricate devices with and without this insulating layer will help resolve the question. The Nb cap is then sputter deposited and defined by lift-off. This also creates holes in the Nb cap so that the Au absorber can directly contact the Ag:Er for good thermal coupling and thus increased detector speed (Figure 9).

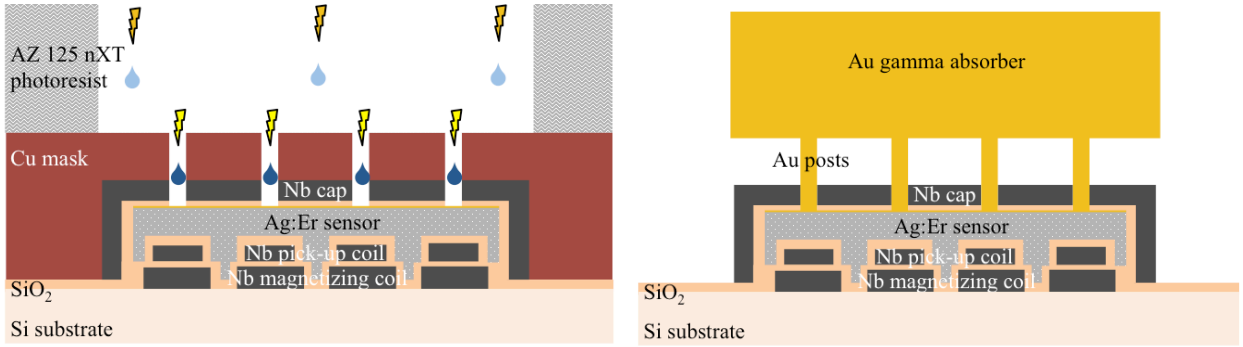

Figure 10 (left): MMC cross-section after Ag:Er sensor deposition, patterning of the Cu masks for the Au posts and the AZ-125-nXT photoresist mold for the Au absorber. The flashes and drops symbolize the acid etch to pattern the Cu and the developer to pattern the AZ-125-nXT photoresist. Figure 11 (right): Cross section of the completed MMC after electroplating the Au absorber and removal of the Cu mask and the photoresist mold.

To ensure full thermalization of the gamma energy inside the absorber, the Au absorber must be separated from the Ag:Er sensor by a set of 25 µm diameter Au posts. One difficulty is that this process requires two different photoresists to be patterned on top of each other, one for the posts, and another thick one for the Au absorber. However, the AZ-125-nXT photoresist required for the thick absorber contains a large number of solvents that attack commercial photoresists underneath[1]. We have solved this problem by replacing the lower photoresist with a 5 µm thick sacrificial Cu mask layer (Figure 10). This Cu mask can be etched with a standard commercial Cu etch (Transene APS 100, 15-20% ammonium peroxydisulfate), using the Au layer as an etch stop, to form the hole pattern for the posts. The Cu is not attacked by the solvents in the AZ-125-nXT photoresist on top of it, nor by the acetone that is used to remove it.

We spin AZ-125-nXT photoresist onto the patterned Cu mask at 1500 rpm for a total thickness of ~300 µm, and pre-bake it for 1 hour at 105 ˚C in a covered and leveled container. We have found it difficult to bake enough solvents out of the photoresist to prevent it from sticking to the photomask without drying it to the point that it can no longer be developed reliably. We therefore add a thin plastic film on top of the AZ-125-nXT before UV exposure, which is removed before forming the mold with the AZ-300-MIF developer [Staab 2012].

Since electroplating requires a conducting path for the ions from the solution, we initially sputter deposit a Nb adhesion layer and a Au seed layer onto the AZ-125-nXT photoresist mold. The Au posts and absorber and then electroplated from a solution with a Au concentration of 8.2 g/l at a current density of 2.5 mA/cm^2 for a rate of 158 nm/minute. For lowest film stress, we have built a custom-designed current source to repeatedly apply the electroplating current for 500 s, followed by 200 s breaks, according to the recipe of the plating solution's manufacturer (Technic). We have successfully deposited Au absorbers to a thickness to 100 µm, and expect to be able to increase the thickness to >200 µm if desired for higher quantum efficiency. The optimized plating process produces a high-quality Au absorber with a residual resistance ratio (RRR) of >25, indicating that the impurity concentration is very low as needed for rapid thermal equilibration of the gamma-ray energy throughout the absorber. Finally, the AZ-125-nXT mold and the sacrificial Cu layer are removed, so that the Au absorber is only supported by the thin Au posts (Figure 11). A picture of a completed detector test device is shown in figure 12.

[1] The one photoresist that is not attacked by AZ-125-nXT is SU-8. However, SU-8 can only be dissolved in "Piranha etch" (3:1 H_2SO_4:H_2O_2), which damages other parts of the MMC detector.

Next Steps

The fabrication process now produces devices with high yield. We have tested the different fabrication steps and the different components of the MMC individually, and optimized the process so that they all meet their required specifications: The SQUID performance is not affected by the fabrication of the MMC on the same chip, the critical current of the Nb coil and the passive Ta-Nb heat switch is sufficient to allow magnetizing currents above 100 mA (Figure 13, 14), and the insulating layers between the different components are pinhole-free and survive repeated thermal cycling. The photolithographic design is scalable to large array sizes, and we have significant flexibility to adjust the geometry and the design parameters. The next step is to test the completed devices, both their equilibrium properties and their response to gamma rays. Most likely, these tests will show certain differences from the literature values that we have assumed in the design of the initial devices, and will require some additional fine-tuning for optimized performance. Once initial samples have been characterized and the fabrication process has been fine-tuned, this report will likely form the basis for a paper on MMC fabrication.

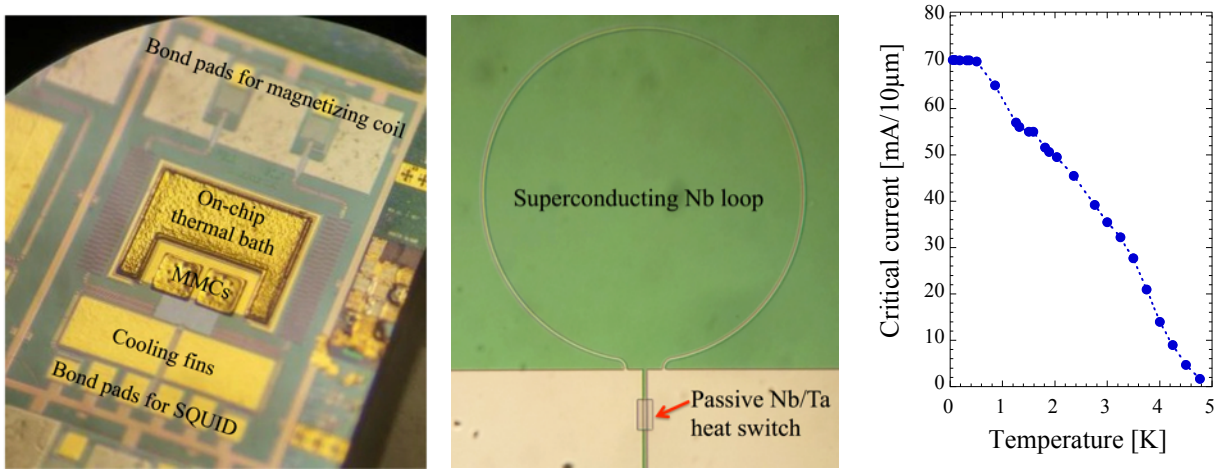

Figure 12 (left): Picture of a completed MMC test device with the Au absorber. The Au posts on the spiral coil are visible as rings of dots in the Au absorber of the MMCs. Figure 13 (center): The new passive Nb-Ta heat switch is extremely simple and reliable. Figure 14 (right): Measurements of the critical current of a 10 μm wide heat switch show that a width of 100 μm is sufficient for a current carrying capability >100 mA at ≤4 K.

References

[Bates 2014] "Development of MMC Gamma Detectors for Nuclear Analysis", C. R. Bates, C. Pies, S. Kempf, L. Gastaldo, A. Fleischmann, C. Enss, S. Friedrich, *J. Low Temp. Phys.* **176**, 631–636 (2014) DOI 10.1007/s10909-013-1063-7

[Boyd 2009] "Microcalorimeter Magnetic Sensor Geometries Using Superconducting Elements", S.T.P. Boyd, R.H. Cantor, *AIP Conference Proceedings* **1185**, 595–598 (2009)

[Jaeckel 2012] "Dedicated Co-deposition System for Metallic Paramagnetic Films", F. Jaeckel, V. Kotsubo, J.A. Hall, R. Cantor, S.T.P. Boyd, *J. Low Temp. Phys* **167**, 286–291 (2012) DOI 10.1007/s10909-012-0564-0

[Staab 2011] "Applications of novel high-aspect-ratio ultra-thick UV photoresist for micro-electroplating", M. Staab, F. Greiner, M. Schlosser, H.F. Schlaak, *JMEMS Lett.* **20**(4), 794–796 (2011)